# Space charge limited current mechanism in Bi$_2$S$_3$ nanowires

Gunta Kunakova,[1] Roman Viter,[2] Simon Abay,[3,4] Subhajit Biswas,[5] Justin D. Holmes,[5] Thilo Bauch,[3] Floriana Lombardi,[3] and Donats Erts[1,a)]

[1]*Institute of Chemical Physics, University of Latvia, Raina Blvd. 19, LV-1586 Riga, Latvia*
[2]*Institute of Atomic Physics and Spectroscopy, University of Latvia, Raina Blvd. 19, LV-1586 Riga, Latvia*
[3]*Quantum Device Physics Laboratory, Department of Microtechnology and Nanoscience, Chalmers University of Technology, SE-41296 Göteborg, Sweden*
[4]*Department of Solid State Physics, Lund University, Lund, Sweden*
[5]*Department of Chemistry and the Tyndall National Institute, University College Cork, Cork, Ireland*

We report on the charge transport properties of individual Bi$_2$S$_3$ nanowires grown within the pores of anodized aluminum oxide templates. The mean pore diameter was 80 nm. Space charge limited current is the dominating conduction mechanism at temperatures below 160 K. Characteristic parameters of nanowires, such as trap concentration and trap characteristic energy, were estimated from current–voltage characteristics at several temperatures. © 2016 AIP Publishing LLC.
[http://dx.doi.org/10.1063/1.4944432]

## I. INTRODUCTION

Nanostructured materials, such as nanowires, have been extensively studied during the last decade. Several functional devices, e.g., solar cells and chemical sensors,[1,2] look promising. There are recent initiatives for the integration of bottom-up grown nanowires in large scale devices. One of the most important and relevant among them is a nano-assembling technique,[3] which can produce nanowires with very few crossing defects and a high precision of alignment. This technique was successfully employed to fabricate highly organized, integrated computational circuits from large scale nanowire assemblies.[4]

With the first demonstration of a memristor based on drift of oxygen vacancies in TiO$_2$ thin films,[5] remarkable attention has been devoted to nanowire based resistive random access memory devices and memristors. Metal/insulator/metal structures have been successfully engineered, employing various types of nanowires, such as Ga$_2$O$_3$, VO$_2$, or Ag$_2$S,[6–8] and provide switching between the low and high resistance states in the current-voltage characteristics. A space charge limited current (SCLC) is one of the conduction mechanisms used to explain the carrier migration phenomena responsible for the resistive switching, as recently observed in ZnO nanorods,[9] as well as in Ga$_2$O$_3$ and CuO$_x$ nanowires.[6,10] SCLC occurs when the rate of recombination of the electrons injected into the conduction band (or holes into the valence band) exceeds the concentration of the initial charge carriers.[11]

The SCLC transport strongly depends on the characteristic parameters of the charge traps. These can be evaluated from the peculiar current–voltage characteristics. The SCLC approach to study the characteristic parameters of individual nanowires, such as concentration of charge traps and their activation energy, from current–voltage characteristics has been discussed recently.[12–15]

Bismuth sulfide (Bi$_2$S$_3$) is a direct band gap semiconductor (E$_g$–1.3 eV) with n-type conduction. It has a great potential for application in resistive memory devices due to its specific intrinsic doping with sulfur vacancies that can play a key role in resistive switching.[16] Numerous approaches have been used to obtain Bi$_2$S$_3$ with excess sulfur or deficiency that can be easily tuned during the growth or by annealing procedures in an appropriate atmosphere.[16–19]

In this article, we report the electrical characterization of individual Bi$_2$S$_3$ nanowires grown in an anodized aluminum oxide, AAO, template via thermal decomposition. The temperature dependent current–voltage characteristics (IVCs) of the nanowires indicate that an SCLC mechanism dominates over Ohmic conduction at temperatures below 160 K. To the best of our knowledge, SCLC has not been previously reported for Bi$_2$S$_3$. Here, we have focused on the characteristic parameters of traps in the Bi$_2$S$_3$ nanowires.

## II. EXPERIMENTAL

Bi$_2$S$_3$ nanowires were grown inside the pores of anodized aluminum oxide templates by thermal decomposition of a single source precursor as previously reported.[20] Both sides of samples were mechanically polished using diamond suspension paste with a particle size between 6 and 0.5 $\mu$m to remove the reaction products formed on top of the nanowire membrane. Selective chemical etching of the polished Bi$_2$S$_3$/AAO membranes was carried out in 9% H$_3$PO$_4$ solution to free the nanowires from the templates.[21,22]

Thus, a suspension containing Bi$_2$S$_3$ nanowires and Al$_2$O$_3$ dissolution products was prepared. Further steps of centrifugation (500 rpm, 1 min × 5) were applied to transfer the nanowires from a H$_3$PO$_4$ solution to isopropanol. The nanowire/isopropanol suspension was drop-cast onto a pre-patterned oxidized silicon substrate and dried using a compressed N$_2$ flow. Individual nanowires were selected for device fabrication. Electrical contacts were patterned using an electron beam lithography (JEOL JBX-9300FS) with a

a)Electronic mail: donats.erts@lu.lv

bilayer ZEP 520/PMMA-MMA resist followed by the evaporation of 3 nm Ti and 80–100 nm Au or Al layers. After the lift off in hot acetone, the samples were additionally cleaned in an oxygen plasma (50 W, 5 s, and 40 sccm).

Two and four point electrical measurements were performed in a ³He refrigerator (300 mK Heliox system) to measure the temperature dependent current-voltage characteristics. Two outer contacts were used as current electrodes, while two inner contacts were used to measure the voltage drop across the nanowire.

## III. RESULTS AND DISCUSSION

Figure 1(a) shows a scanning electron microscope SEM image of an electrically contacted individual $Bi_2S_3$ nanowire. Figure 1(b) highlights the nonlinear IVCs obtained from three $Bi_2S_3$ nanowires. For all three wires, no surface treatment was performed on the nanowires prior to the deposition of the electrical contacts. The IVCs were typically nonlinear with symmetric, asymmetric, or rectifying behavior (Figure 1(b)). Nonlinear IVCs at room temperature for $Bi_2S_3$ nanowire devices have previously been explained by a metal (M)–semiconductor (S)–metal (M) model, providing Schottky barriers' formation at the M-S interface.[23] In the presence of Schottky emission, the IVC follows the relationship $\ln(I) = A + BV^{(1/2)}$, where A and B (B > 0) are constants[24] and $I$ is the current through the device and $V$ is the voltage across the device. Examples of data plotted as $\ln(I)$ versus $V^{1/2}$ are shown in the inset of Figure 1(b). As one can see, the data follow a linear fit at voltages below 0.25 V, indicating Schottky emission.

One possibility to fabricate $Bi_3S_3$ nanowire devices exhibiting linear IVCs is post-annealing of the nanowire samples as described in Ref. 18. In our work, Ohmic contacts with linear IVCs were obtained by etching of the nanowire contact areas in ammonium polysulfide water solution $(NH_4)_2S_n \div H_2O \,(1 \div 9)$ at 40 °C, 5 min before metal deposition (Figure 1(c)).

To determine the contact resistance, IVCs of different lengths between the contacts of the nanowire were measured in a two-electrode configuration. The resistance depends linearly on the nanowire length (Figure 1(d)). The $y$ intercept of the linear fit (about 0.4 MΩ) corresponds to 2 $R_c$, where $R_c$ is the contact resistance. From the estimated contact resistance $R_c$, one can get the mean resistivity at room temperature for individual $Bi_2S_3$ nanowires. In our experiment, we have obtained a value of about 0.01 Ωm, which is one order of magnitude lower than that previously reported.[25] Unlike previous reports, electrical measurements were performed under vacuum, so as to minimize the effect of humidity on the carrier transport properties of the nanowires.[26]

Figure 2(a) shows several IVCs for $Bi_2S_3$ nanowires as a function of temperature. A linear behavior was observed only at 295 K; IVCs became strongly nonlinear as the temperature fell below 240 K. To determine the mechanism responsible for the nonlinear characteristics, the data were fitted using several conduction models for semiconductors and insulators.

Assuming a difference in the electrical properties between the surface and the bulk of a nanowire at temperatures below 240 K, the Fowler-Nordheim conduction mechanism can be considered. In this case, a straight line is expected for IVC data when plotting $\ln I/V^2 \sim 1/V^2$.[11] For
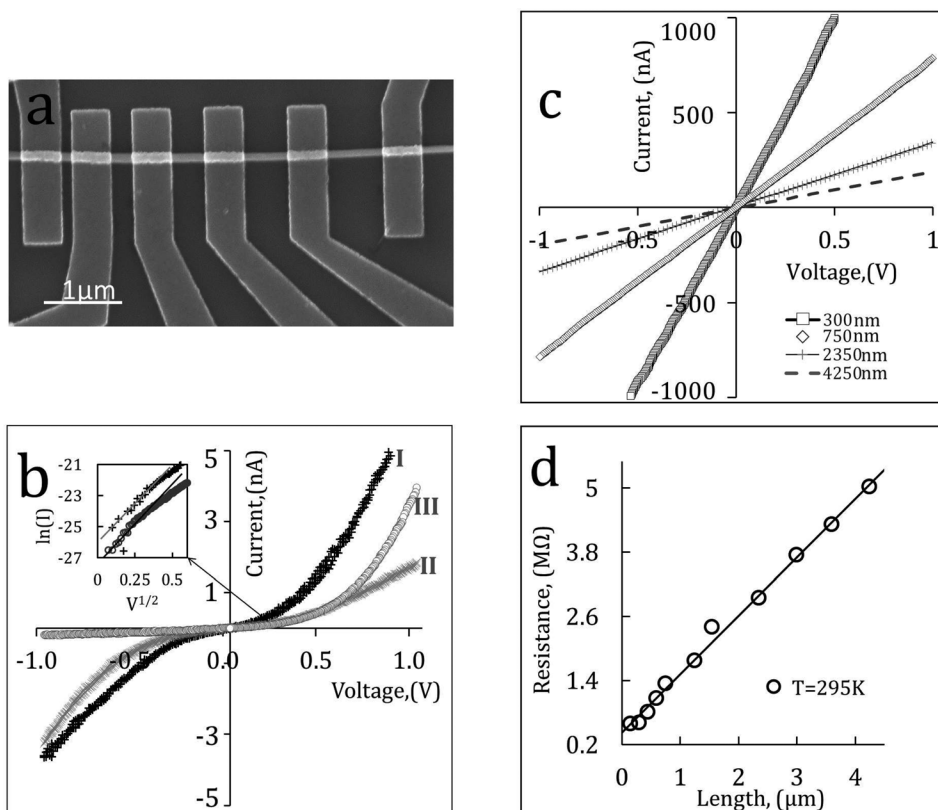


FIG. 1. (a) SEM image of a $Bi_2S_3$ nanowire device with diameter d = 80 nm; (b) nonlinear IVCs measured at room temperature in a two electrode configuration showing symmetric I, asymmetric II and rectifying III behavior for nanowires without contact area etching; (c) linear IVCs of $Bi_2S_3$ nanowire with etched contact areas measured at different distances between the electrodes (d = 80 nm), room temperature; (d) resistance of the $Bi_2S_3$ nanowire as a function of length at room temperature.
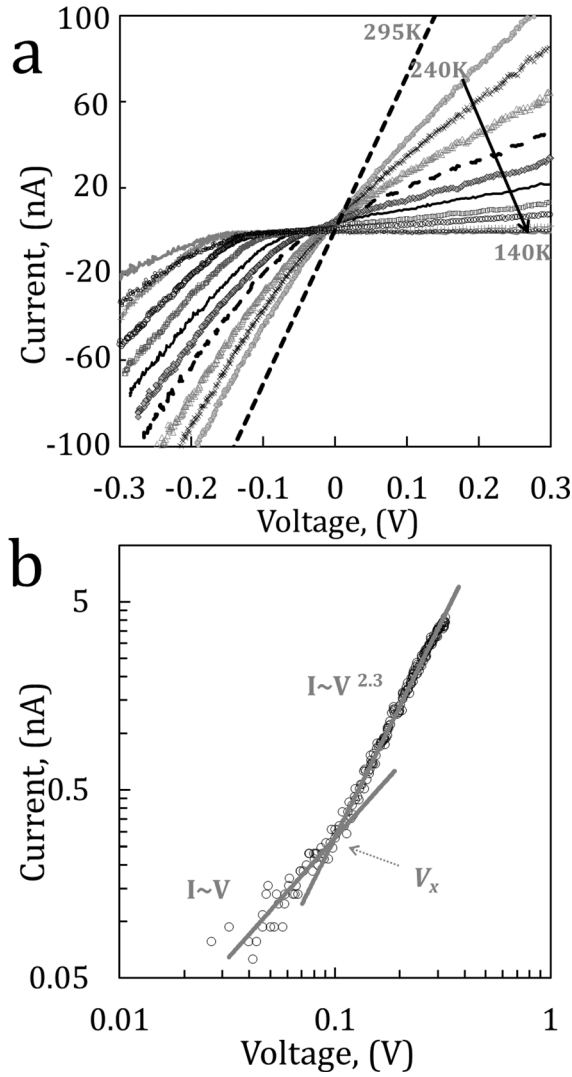
FIG. 2. (a) Temperature dependent IVCs at 295 K and 240–140 K, nanowire length between electrodes 300 nm, d = 80 nm; (b) log-log plots of the IVC at T = 150 K.

curves exhibiting Schottky behavior the IVC should follow $\ln(I) \sim V^{1/2}$ in the low voltage region as we show in the inset of Figure 1(b). A Frenkel-Poole model, which describes carrier emission from trapped states, was also considered, and a straight line fit would be expected for $\sinh^{-1}(I/V)$ versus $\sqrt{V}$.[11] However, the Fowler-Nordheim, Schottky emission, and Frenkel-Poole models did not fit our data.

Instead, an $I \sim V^n$ ($n = 1$–3.5) dependence was observed over the temperature range between 130 and 300 K in both positive and negative branches of the IVCs, with an increase in the exponent ($n$) values as the temperature decreases. An $I \sim V^n$ with $n \geq 2$ dependence of IVCs below 160 K indicates a dominant space charge limited current. SCLC injection has previously been reported as a leading transport mechanism for GaAs nanowires in specific temperature intervals of $\sim$250–160 K (Ref. 12) and at room temperature for AlGaN/GaN nanowires.[13]

In the presence of charge traps, the IVC dominated by SCLC reflects the properties of the traps and therefore can be used as a charge trap characterization tool.[12,27,28]

Figure 2(b) represents one example of the IVC of a $Bi_2S_3$ nanowire at 150 K (plotted on a log-log scale), where $I \sim V^{2.3}$ was observed at $V > 0.1$ V. The IVC at a temperature of 150 K was used to evaluate the free carrier concentration. At a voltage below 0.1 V, the IVC follows Ohm's law ($I \sim V$), but above 0.1 V, the SCLC mechanism is charge transfer dominated. The value of the voltage where the SCLC starts to dominate over the Ohmic conduction is denoted as the crossover voltage $V_x$.[29] At $V_x$, the injected carrier concentration (n) reaches the value of the free carrier concentration ($n_0$) and the relationship between $V_x$ and the free carrier density for cylindrical nanowires can be estimated[13] from equation

$$n_0 = \frac{V_x \varepsilon}{q r^2}, \quad (1)$$

where $r$ and $\varepsilon$ are the nanowire radius and the dielectric constant of the semiconductor, respectively; $q$ is the charge of the electron. Using a voltage $V_x = 0.1$ V (Figure 2(b)), the calculated free carrier density was determined to be $4.3 \times 10^{16}$ cm$^{-3}$, which is comparable with values determined by Hall effect measurements at low temperature for $Bi_2S_3$ single crystals.[30]

Transmission Raman spectroscopy may be used to extract the carrier concentration of individual nanowires as a non-electrical validation[31] or, alternatively, infrared reflectivity measurements for nanowire arrays. To the best of our knowledge, non-electrical estimates of the carrier concentration of individual $Bi_2S_3$ nanowires have not been performed. However, similar experiments have been reported for other bismuth chalcogenide crystals of $Bi_2Se_3$.[32] Reported values of carrier density determined by both non-electrical and electrical measurements correspond well, we therefore assume that similar trend may be observed also for $Bi_2S_3$.

We plot the exponent $n$ extracted from the IVCs at various temperatures as a function of $1/T$ in Figure 3(a). At temperatures T > 190 K, $n \sim 1$, which can be attributed to Ohmic conduction followed by a transition to the SCLC regime as $l + 1 \geq 2$ at temperatures below 160 K. The temperature dependence of the exponent $n$ (see Figure 3(a)) strongly indicates that the trap distribution is exponential in an energy gap: $\exp(-E/kT_t)$, where $E$ is measured from the bottom of the conduction band.[33] Here, $kT_t = E_{ct}$ is the characteristic energy of the trap distribution and $k$ is the Boltzmann constant. Following Ref. 33, the exponent $n$ below 160 K can be rewritten as $n = l + 1$, where $l$ is given by the ratio $l = T_t/T$.

For traps with exponential energy distribution, the space charge limited current density is given by[33]

$$J = q^{(1-l)} \mu N_c \left( \frac{2l+1}{l+1} \right)^{l+1} \left( \frac{l}{l+1} \frac{\varepsilon}{H} \right)^l \frac{V^{l+1}}{L^{2l+1}}. \quad (2)$$

Here, $\mu$ is the electron mobility; $N_c$ is the effective density of states in the conduction band; $H$ is the trap concentration; $\varepsilon$ is the dielectric constant; and $L$ is distance between the electrodes.

In order to determine the trap characteristic energy $E_{ct}$, we have analyzed the temperature dependence of the voltage exponent.
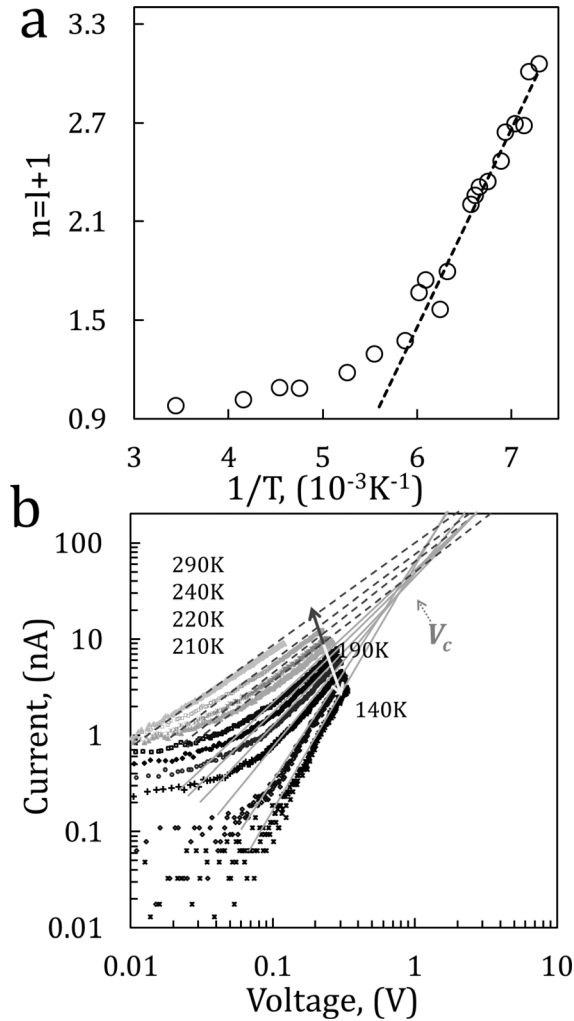
FIG. 3. (a) Voltage scaling exponent as a function of temperature, all determined values of the exponents correspond to the voltage V > 0.1 V; (b) log-log plot of the temperature dependent IVCs.

From the slope of $n = l + 1$ versus 1/T plot (Figure 3(a)) in the SCLC dominated region (T < 160 K), we have obtained a value of the characteristic trap temperature of 1108 K, which according to the expression $E_{ct} = kT_t$[33] gives a characteristic charge trap energy of the order of 100 meV.

It is not possible to determine a direct origin of the charge traps in the SCLC model. We may exclude extrinsic impurities acting as charge traps in our catalyst free synthesis method to fabricate nanowires. Most likely, these existing trapping centers in $Bi_2S_3$ nanowires at low temperatures can be attributed to structural defects.

In order to establish the concentration of the traps with exponential energy distribution, the common approach involves the derivation of the crossover voltage ($V_c$) related to the trap concentration (H) as[34]

$$V_c = \frac{qHL^2}{2\varepsilon\varepsilon_0}.$$ (3)

The crossover voltage can be determined by extrapolating temperature dependent IVCs in log-log plots to high voltages where the curves influenced by SCLC should exhibit a crossing point. Our data in the temperature range from 290 to

210 K do not exhibit any crossover. At lower temperatures, however, IVCs unveil $V_c = 0.9$ V (Figure 3(b)). Using this value, the calculated density of the traps is $1.2 \times 10^{16}$ cm$^{-3}$ (using a value of $\varepsilon = 11$ (Ref. 30)).

Trap characteristics for $Bi_2S_3$ nanocrystals at room temperature have recently been determined by time resolved spectroscopy. An overall trap density of the order of $10^{20}$ cm$^{-3}$ was assigned to the contribution of surface states caused by incomplete surface passivation.[35] From our data, the calculated trap concentration is of the order of $10^{16}$ cm$^{-3}$. Thus, it can be concluded that the determined trap concentration at temperatures below 160 K could originate from the nanowire bulk.

In order to access the distribution of energies of the traps at the surface of a $Bi_2S_3$ nanowire, the current-voltage characteristics measured at higher voltages are required. The corresponding trap concentration at the nanowires surface can be expected to be considerably higher compared to the trap concentration in the nanowire bulk. Therefore, the value of the crossover voltage will be higher. However, the measurements of the current-voltage curves at higher voltages may cause a degradation of the nanowire. Gas molecules such as $O_2$ and $H_2O$ may be used in alternative surface treatment methods to achieve a decreased density of the trap states.

It is important to increase the temperature at which the SCLC dominates for a practical realization of $Bi_2S_3$ nanowire based memristors. A memristor of Au/ZnO nanorods/conductive glass operating in the SCLC mode at room temperature was recently demonstrated.[9] The active ZnO nanorods are of a similar scale as our $Bi_2S_3$ nanowires, and the elements showed excellent stability of resistive switching.[9] By tuning device geometry (e.g., the diameter of the nanowire and its length between the electrodes) and optimizing surrounding environment, SCLC may be observed also at room temperature in $Bi_2S_3$ nanowires.

## IV. CONCLUSIONS

We have shown how to control the contact properties of $Bi_2S_3$ nanowires by suitable treatment of the electrode–nanowire interface. We have analyzed the charge carrier transport in $Bi_2S_3$ nanowires. The SCLC conduction mechanism is found to dominate at temperatures below 160 K. By a careful analysis of IVCs affected by SCLC, we have been able to determine the shallow charge traps with an exponential distribution of energy with a concentration of the order of $1 \times 10^{16}$ cm$^{-3}$. The determined concentration of traps is rather high. This could enhance the on/off ratio of the resistive switching.

The understanding of nanowire transport properties at different temperatures is critical for their integration in electronic devices. The observation of the SCLC mechanism enables further investigations for nanowire application in the resistive switching devices.

We believe that the advancement of these techniques will be beneficial for integration of bottom-up grown chalcogenide nanowires in large scale devices showing SCLC at room temperature.

[1]B. Tian, X. Zheng, T. J. Kempa, Y. Fang, N. Yu, G. Yu, J. Huang, and C. M. Lieber, "Coaxial silicon nanowires as solar cells and nanoelectronic power sources," Nature **449**, 885–889 (2007).

[2]M. C. McAlpine, H. Ahmad, D. Wang, and J. R. Heath, "Highly ordered nanowire arrays on plastic substrates for ultrasensitive flexible chemical sensors," Nat. Mater. **6**, 379–384 (2007).

[3]J. Yao, H. Yan, and C. M. Lieber, "A nanoscale combing technique for the large-scale assembly of highly aligned nanowires," Nat. Nanotechnol. **8**, 329–335 (2013).

[4]J. Yao, H. Yan, S. Das, J. F. Klemic, J. C. Ellenbogen, and C. M. Lieber, "Nanowire nanocomputer as a finite-state machine," Proc. Natl. Acad. Sci. U. S. A. **111**, 2431–2435 (2014).

[5]J. J. Yang, M. D. Pickett, X. Li, D. A. A. Ohlberg, D. R. Stewart, and R. S. Williams, "Memristive switching mechanism for metal/oxide/metal nano-devices," Nat. Nanotechnol. **3**, 429–433 (2008).

[6]C.-W. Hsu and L.-J. Chou, "Bipolar resistive switching of single gold-in-$Ga_2O_3$ nanowire," Nano Lett. **12**, 4247–4253 (2012).

[7]S.-H. Bae, S. Lee, H. Koo, L. Lin, B. H. Jo, C. Park, and Z. L. Wang, "The memristive properties of a single $VO_2$ nanowire with switching controlled by self-heating," Adv. Mater. **25**, 5098–5103 (2013).

[8]Z.-M. Liao, C. Hou, Q. Zhao, D.-S. Wang, Y.-D. Li, and D.-P. Yu, "Resistive switching and metallic-filament formation in $Ag_2S$ nanowire transistors," Small **5**, 2377–2381 (2009).

[9]Y. Sun, X. Yan, X. Zheng, Y. Liu, Y. Zhao, Y. Shen, Q. Liao, and Y. Zhang, "High on–off ratio improvement of ZnO-based forming-free memristor by surface hydrogen annealing," ACS Appl. Mater. Interfaces **7**, 7382–7388 (2015).

[10]K.-D. Liang, C.-H. Huang, C.-C. Lai, J.-S. Huang, H.-W. Tsai, Y.-C. Wang, Y.-C. Shih, M.-T. Chang, S.-C. Lo, and Y.-L. Chueh, "Single $CuO_x$ nanowire memristor: Forming-free resistive switching behavior," ACS Appl. Mater. Interfaces **6**, 16537–16544 (2014).

[11]K. C. Kao, *Dielectric Phenomena in Solids: With Emphasis on Physical Concepts of Electronic Processes* (Elsevier Academic Press, 2004).

[12]A. D. Schricker, F. M. Davidson, R. J. Wiacek, and B. A. Korgel, "Space charge limited currents and trap concentrations in GaAs nanowires," Nanotechnology **17**, 2681–2688 (2006).

[13]B. S. Simpkins, M. A. Mastro, C. R. Eddy, J. K. Hite, and P. E. Pehrsson, "Space-charge-limited currents and trap characterization in coaxial AlGaN/GaN nanowires," J. Appl. Phys. **110**, 044303–044304 (2011).

[14]W. Xu, A. Chin, L. Ye, C. Z. Ning, and H. Yu, "Charge transport and trap characterization in individual GaSb nanowires," J. Appl. Phys. **111**, 104515 (2012).

[15]D. Ko, X. W. Zhao, K. M. Reddy, O. D. Restrepo, R. Mishra, T. R. Lemberger, I. S. Beloborodov, N. Trivedi, N. P. Padture, W. Windl, F. Y. Yang, and E. Johnston-Halperin, "Defect states and disorder in charge transport in semiconductor nanowires," J. Appl. Phys. **114**, 043711 (2013).

[16]D. Guo, C. Hu, and C. Zhang, "First-principles study on doping and temperature dependence of thermoelectric property of $Bi_2S_3$ thermoelectric material," Mater. Res. Bull. **48**, 1984–1988 (2013).

[17]H. Rau, "Range of homogeneity and defect model," J. Phys. Chem. Solids **42**, 257–262 (1981).

[18]A. D. Schricker, M. B. Sigman, and B. A. Korgel, "Electrical transport, Meyer–Neldel rule and oxygen sensitivity of $Bi_2S_3$ nanowires," Nanotechnology **16**, S508–S513 (2005).

[19]H. Mizoguchi, H. Hosono, N. Ueda, and H. Kawazoe, "Preparation and electrical properties of $Bi_2S_3$ whiskers," J. Appl. Phys. **78**, 1376 (1995).

[20]J. Xu, N. Petkov, X. Wu, D. Iacopino, A. J. Quinn, G. Redmond, T. Bein, M. A. Morris, and J. D. Holmes, "Oriented growth of single-crystalline $Bi_2S_3$ nanowire arrays," ChemPhysChem **8**, 235–240 (2007).

[21]D. Erts, B. Polyakov, B. Daly, M. A. Morris, S. Ellingboe, J. Boland, and J. D. Holmes, "High density germanium nanowire assemblies: Contact challenges and electrical characterization," J. Phys. Chem. B **110**, 820–826 (2006).

[22]N. Petkov, P. Birjukovs, R. Phelan, M. A. Morris, D. Erts, and J. D. Holmes, "Growth of ordered arrangements of one-dimensional germanium nanostructures with controllable crystallinities," Chem. Mater. **20**, 1902–1908 (2008).

[23]H. Bao, C. M. Li, X. Cui, Y. Gan, Q. Song, and J. Guo, "Synthesis of a highly ordered single-crystalline $Bi_2S_3$ nanowire array and its metal/semi-conductor/metal back-to-back Schottky diode," Small **4**, 1125–1129 (2008).

[24]Y. Tian, C. Guo, S. Guo, T. Yu, and Q. Liu, "Bivariate-continuous-tunable interface memristor based on $Bi_2S_3$ nested nano-networks," Nano Res. **7**, 953–962 (2014).

[25]P. Birjukovs, N. Petkov, J. Xu, J. Svirksts, J. J. Boland, J. D. Holmes, and D. Erts, "Electrical characterization of bismuth sulfide nanowire arrays by conductive atomic force microscopy," J. Phys. Chem. C **112**, 19680–19685 (2008).

[26]G. Kunakova, R. Meija, I. Bite, J. Prikulis, J. Kosmaca, J. Varghese, J. D. Holmes, and D. Erts, "Sensing properties of assembled $Bi_2S_3$ nanowire arrays," Phys. Scr. **90**, 094017 (2015).

[27]A. Talin, F. Léonard, B. Swartzentruber, X. Wang, and S. Hersee, "Unusually strong space-charge-limited current in thin wires," Phys. Rev. Lett. **101**, 076802–076804 (2008).

[28]K. Rasool, M. A. Rafiq, M. Ahmad, Z. Imran, and M. M. Hasan, "The role of surface states in modification of carrier transport in silicon nanowires," J. Appl. Phys. **113**, 193703–193705 (2013).

[29]M. Lampert, "Volume-controlled current injection in insulators," Rep. Prog. Phys. **27**, 329–367 (1964).

[30]A. Cantarero, J. Martinez-Pastor, A. Segura, and A. Chevy, "Transport properties of bismuth sulfide single crystals," Phys. Rev. B **35**, 9586–9590 (1987).

[31]B. Ketterer, E. Uccelli, and A. Fontcuberta i Morral, "Mobility and carrier density in p-type GaAs nanowires measured by transmission Raman spectroscopy," Nanoscale **4**, 1789–1793 (2012).

[32]C. Julien, I. Samaras, and A. Chevy, "Studies of lithium insertion in bismuth chalcogenide compounds," Solid State Ionics **36**, 113–120 (1989).

[33]P. Mark and W. Helfrich, "Space-charge-limited currents in organic crystals," J. Appl. Phys. **33**, 205–215 (1962).

[34]V. Kumar, S. C. Jain, A. K. Kapoor, J. Poortmans, and R. Mertens, "Trap density in conducting organic semiconductors determined from temperature dependence of JV characteristics," J. Appl. Phys. **94**, 1283 (2003).

[35]M. Aresti, M. Saba, R. Piras, D. Marongiu, G. Mula, F. Quochi, A. Mura, C. Cannas, M. Mureddu, A. Ardu, G. Ennas, V. Calzia, A. Mattoni, A. Musinu, and G. Bongiovanni, "Colloidal $Bi_2S_3$ nanocrystals: Quantum size effects and midgap states," Adv. Funct. Mater. **24**, 3341–3350 (2014).